ELSEVIER

Chemical Engineering Journal 80 (2000) 257–265

Chemical Engineering Journal

www.elsevier.com/locate/cej

Axial symmetric flow model for a flat bottom hydrocyclone

J. Collantes [a], F. Concha [b,*], B. Chiné [c]

[a] *Department of Mathematical Engineering, University of Concepción, Casilla 53 C, Correo 3, Concepción, Chile*
[b] *Department of Metallurgical Engineering, University of Concepción, Casilla 53 C, Correo 3, Concepción, Chile*
[c] *Faculty of Engineering, Catholic University of Concepción, Concepción, Chile*

Abstract

Experiments with laser Doppler velocimetry show that, for flat bottom hydrocyclones, the axial velocity field is a function of the radius and a linear function of the axial co-ordinate, while the tangential velocity is a function of the radial co-ordinate only. Based on these results, a physical model is presented, where the flow field is divided in two zones. Zone I corresponds to the feed inlet, which occurs through a ring in the upper portion of the cylinder, the length of which depends on the length of the vortex finder tube. Zone II includes the rest of the cylinder. The axial symmetric solution of Reynolds equations for the isotropic turbulent flow leads to two sets of field equations, one for each zone in the hydrocyclone. In zone II, where experimental data were determined, simulation compares favourably with the flow pattern determined experimentally for water in a 100-mm flat bottom hydrocyclone.

Keywords: Vortex motion; Hydrocyclone; Mathematical modeling; Fluid dynamics; Axial symmetry

1. Introduction

It is interesting to notice that while, conical hydrocyclones are the most widely used classification equipment in the mineral industries, cylindrical hydrocyclones, more often called flat bottom hydrocyclones, were the first to be mathematically modelled. The reason for this is that the cylindrical geometry is more amenable to mathematical treatment than the cylindro-conical combination. Rietema and co-workers [1–3] modelled the hydrocyclone as a cylindrical device using cylindrical co-ordinates. Assuming axial symmetry, they considered that the feed entered the equipment through the entire cylindrical mantel with an independent combination of a radial velocity component V_R and tangential velocity component $V_{\theta R}$ (see Fig. 1). Since the only experimental information available on the velocity distribution in a hydrocyclone was that of Kelsall [4] for a conical hydrocyclone, Rietema and co-workers, based their work on the flow pattern determined experimentally for conical hydrocyclones, without suspecting that these pattern were different from those of cylindrical hydrocyclones.

The early work on cylindrical hydrocyclones was fragmentary and restricted, in the sense that only the tangential velocity component was studied, assuming that it was a function of the radial co-ordinate only and that the functional form of the radial velocity could be derived from experimental evidence. The consequence of this assumption was not investigated further. As examples, take the cases analysed by Rietema and Krajenbrink [1], where the radial velocity was assumed to have the form $v_r = RV_R/r$, Rietema [2], who assumed that the radial velocity was constant in the whole flow field $v_r = V_R$ or Rietema [5], who solved the same equation and boundary conditions but now assuming that the radial velocity was a linear function of the radius, $v_r = (V_R/R)r$. In all three cases, they obtained an analytical equation with very similar tangential velocity distributions, except for the value of the radial Reynolds number at which they compared prediction with the experiments of Kelsall. While for Rietema and Krajenbrink [1], this value was $Re \approx 3$, corresponding to a turbulent eddy viscosity of the order of $\nu_\epsilon \approx 10^{-3}$ m^2/s, for Rietema [2], it was $Re \approx 10$, that is, a turbulent eddy viscosity of $\nu_\epsilon \approx 3 \times 10^{-4}$ m^2/s and for Rietema [5] $Re \approx 30$, that is, with a turbulent eddy viscosity of $\nu_\epsilon \approx 10^{-4}$ m^2/s). It is important to point out that Kelsall [4] measured the tangential and the axial velocity component and derived the radial velocity from these measurements and from continuity. His results show that the radial velocity is a linear function of the radial co-ordinate, that is, the way assumed by Rietema [5].

The problem with the models developed by Rietema and co-workers is that they do not consider explicitly the axial velocity, which was experimentally known, and assumed arbitrarily a radial velocity. Furthermore, their solutions serve only to calculate the centrifugal force, but give no clue as to how the particles are separated and how the particles and

* Corresponding author. Fax: +56-41-230759.
E-mail addresses: jcollant@ing-mat.udec.cl (J. Collantes), fconcha@udec.cl (F. Concha).

1383-5866/00/$ – see front matter
PII: S1383-5866(00)00099-X

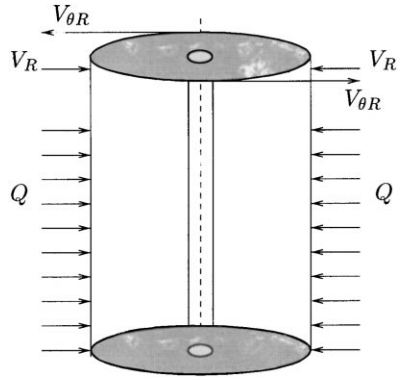

Fig. 1. Axial symmetric model of a cylindrical hydrocyclone according to Rietema and co-workers.

fluid are evacuated from the equipment. The conclusion is that, to solve the dynamic process for cylindrical hydrocyclones, it is first necessary to measure the axial and tangential velocity distributions in these hydrocyclones, and then, it is essential to solve all three components of Reynolds equations, together with the continuity equation. That is the objective of this work.

2. Experimental

2.1. Flow configuration

A flat bottom hydrocyclone 102 mm in diameter and 310.5 mm total in height was built in Perspex. The flow enters the hydrocyclone tangentially through a rectangular tube with 16×43-mm cross section. The hydrocyclone body is a cylinder, 301 mm in length, ending in a short conical section, 9.5 mm in height, forming an angle of 154°. The overflow occurs through a vortex finder tube 82 mm in length and 32 mm in diameter, while the underflow discharge is through an apex of 19 mm in diameter.

Water at room temperature (20±0.5°C) was fed to the hydrocyclone under controlled flow conditions by a set of valves. The fluid was pumped from a 0.665 m^3 sump by means of a 4 hp centrifugal pump. Feed pressure and flow rates were monitored with accurate manometers and rotameters. Finally, to generate tracer particles for the Laser-Doppler velocimeter (LDV) measurements, latex painting particles were added to the fluid.

2.2. Measurements techniques

Velocity and turbulence were measured inside the flat bottom hydrocyclone with a 300 mW two-component fibre optic Dantec LDV. The instrument is controlled by the burst spectrum analysers (BSA) connected to a PC. The equipment is completed by an automatic, computer-controlled, three-direction traverse system. To minimise the optical refraction of the laser beams at curved walls, the flat bottom hydrocyclone was immersed in a water jacket.

Coherent light from an argon-ion laser, with a wavelength in the range of 457–514.5 nm, was directed to a transmitter box for frequency shifting to remove the velocities direction ambiguity and perform colour separation [6]. A Bragg cell splits the light beam into two beams with a 40-MHz frequency shifting. These beams pass through a dispersion prism, which provides two green 514.5-nm, and two blue 488-nm light beams. The shifted and directed beams are led to the output aperture, where fibre manipulators are used to focus the beams into the fibre optic cables. A 160-mm focal length lens probes with a beam intersection angle of 0.236 rad, causes the four beams to intersect. Finally, the collected back-scattered light is separated into green and blue components and is directed onto two photomultipliers.

In order to extract the Doppler frequencies, the Doppler signals are processed in two BSAs, the BSA master for measuring the main component of the velocity and the BSA slave for the other component, which were set to run in a continuous data collection mode. The experimental data were transferred to a computer for processing via an IEEE-488 interface. To measure the velocity and turbulence in the hydrocyclone, the probe was moved and positioned using a highly accurate computer-controlled three components (x–y–z) traverse system. The BurstWare 2.0 software package was used to collect all the data, move the traverse, process the data and present the results.

Velocity data were thus measured on four symmetrical vertical positions chosen on the curved walls (azimuths co-ordinates θ=0, 90, 180, 270°). The laser beams were focused on a median vertical r, z half-plan crossing the cylindrical model, one for each azimuth co-ordinate θ. Six vertical z-measurements levels were chosen on the median vertical plane. In correspondence to a determined z-coordinate,. the first measurement point was placed near the wall of the cyclone and the last point was chosen in the proximity of the air core. A uniform measurement axial step Δz equal to 40 mm and radial steps Δr of 2.7 and 0.675 mm were used. Finally, in all the experimental work a sample of typically 1000 Doppler bursts was taken for each measurement point.

Table 1 gives the design and operating conditions of the flat bottom hydrocyclone used for the velocity measurements.

3. Theory

3.1. Field equations

The complete Reynolds equations, in cylindrical co-ordinates, for the steady axial symmetric flow, with an isotropic turbulence represented by an eddy viscosity, ν_ϵ are:

$$\frac{\partial}{\partial r}(rv_r) + \frac{\partial}{\partial r}(rv_z) = 0 \quad (1)$$

Table 1
Design and operating conditions of the flat bottom hydrocyclone used for the velocity measurements

Hydrocyclone radius R (cm)	5.1
Vortex radius R_o (cm)	1.6
Apex radius R_u (cm)	0.95
Hydrocyclone length L (cm)	31.05
Vortex finder length L_V (cm)	8.2
Supposed feed inlet length L_A (cm)	10.25
Hydrocyclone cylindrical length (cm)	30.1
Hydrocyclone conical length (cm)	0.95
Total feed flowrate, Q (l/s)	1.42
Overflow rate, Q_r (l/s)	1.27
Underflow rate, Q_d (l/s)	0.15
Characteristic parameter, λ	0.106
Pressure, Δp (psi)	4
Outer tangential velocity $V_{\theta R}$ (m/s)	1.3
Reynolds radial number, Re	65
Turbulent eddy viscosity, ν_ϵ (m^2/s)	3.4×10^{-5}

$$v_r\frac{\partial v_r}{\partial r}+v_z\frac{\partial v_r}{\partial z}-\frac{v_\theta^2}{r}=-\frac{1}{\rho}\frac{\partial p}{\partial r}+\nu_\epsilon\frac{\partial}{\partial r}\left[\frac{1}{r}\frac{\partial}{\partial r}(rv_r)+\frac{\partial^2 v_r}{\partial z^2}\right] \quad (2)$$

$$\frac{v_r}{r}\frac{\partial}{\partial r}(rv_\theta)+v_z\frac{\partial v_\theta}{\partial z}=\nu_\epsilon\frac{\partial}{\partial r}\left[\frac{1}{r}\frac{\partial}{\partial r}(rv_\theta)+\frac{\partial^2 v_\theta}{\partial z^2}\right] \quad (3)$$

$$v_r\frac{\partial v_z}{\partial r}+v_z\frac{\partial v_z}{\partial z}=-\frac{1}{\rho}\frac{\partial p}{\partial z}+\nu_\epsilon\left[\frac{1}{r}\frac{\partial}{\partial r}\left(r\frac{\partial v_z}{\partial r}\right)+\frac{\partial^2 v_z}{\partial z^2}\right] \quad (4)$$

Integrating the continuity equation (Eq. (1)) yields:

$$rv_r(r,z)=-\int\frac{\partial v_z(r,z)}{\partial z}r\,\mathrm{d}r+k \quad (5)$$

From the experimental results, it can be safely assumed that for a cylindrical hydrocyclone, the tangential velocity is independent of the axial co-ordinate. With this assumption and from Eq. (3) we can deduce that the radial velocity should also be a function of the radial co-ordinate only. Now, from Eq. (5) it is clear that the axial velocity gradient must be independent of z. The conclusion is that the most general form of the axial velocity v_z (r,z) is (Donaldson and Sullivan [7]):

$$v_z=f(r)z+g(r) \quad (6)$$

Substituting this relationship into Eqs. (1)–(4) yields,

Continuity equation:

$$\frac{1}{r}\frac{\mathrm{d}}{\mathrm{d}r}(rv_r(r))+f(r)=0 \quad (7)$$

Radial component:

$$v_r(r)=\frac{\mathrm{d}v_r(r)}{\mathrm{d}r}-\frac{v_\theta^2(r)}{r}-\nu_\epsilon\frac{\mathrm{d}}{\mathrm{d}r}\left[\frac{1}{r}\frac{\mathrm{d}}{\mathrm{d}r}(rv_r(r))\right]=-\frac{1}{\rho}\frac{\partial p(r,z)}{\partial r} \quad (8)$$

Tangential component:

$$\frac{v_r(r)}{r}\frac{\mathrm{d}}{\mathrm{d}r}(rv_\theta(r))=\nu_\epsilon\frac{\mathrm{d}}{\mathrm{d}r}\left[\frac{1}{r}\frac{\mathrm{d}}{\mathrm{d}r}(rv_\theta(r))\right] \quad (9)$$

Axial component:

$$\left[v_r(r)\frac{\mathrm{d}f(r)}{\mathrm{d}r}+f^2(r)-\frac{\nu_\epsilon}{r}\frac{\mathrm{d}}{\mathrm{d}r}\left(r\frac{\mathrm{d}f(r)}{\mathrm{d}r}\right)\right]z+\left[v_r(r)\frac{\mathrm{d}g(r)}{\mathrm{d}r}+f(r)g(r)-\frac{\nu_\epsilon}{r}\frac{\mathrm{d}}{\mathrm{d}r}\left(r\frac{\mathrm{d}g(r)}{\mathrm{d}r}\right)\right]=-\frac{1}{\rho}\frac{\partial p(r,z)}{\partial z} \quad (10)$$

Eliminating the pressure from Eqs. (8) and (10), the following set of equations is obtained for $f(r)$ and $g(r)$:

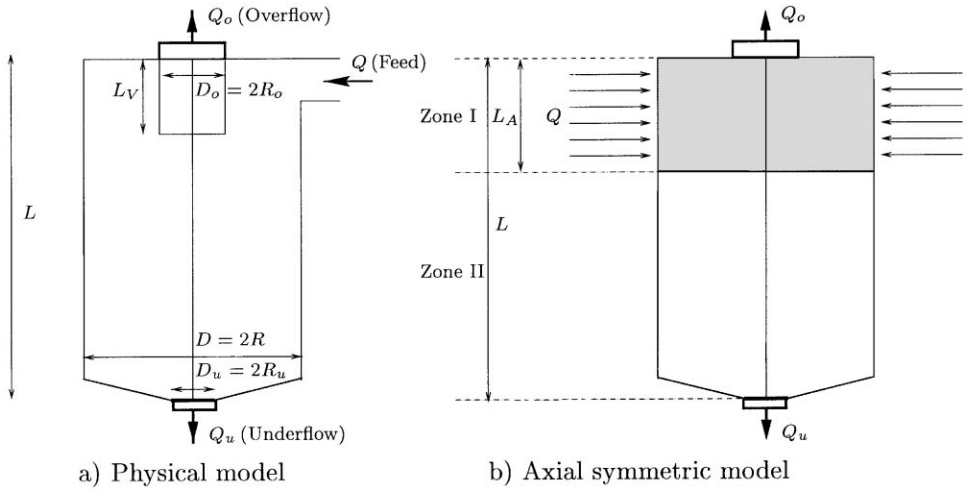

Fig. 2. Schematic representation of the flat bottom hydrocyclone. (a) Physical model; (b) axial symmetric model.

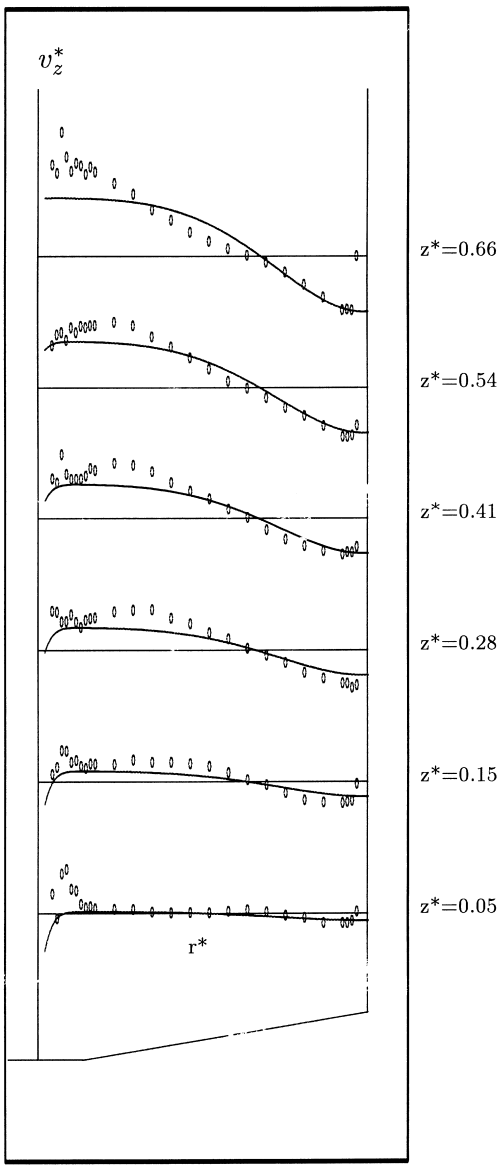

Fig. 3. Comparison of the predicted and experimental dimensionless axial velocity distribution at several axial levels, where $v_z{}^*=v_z/V_{\theta R}$ and $r^*=r/R$.

$$\frac{\mathrm{d}}{\mathrm{d}r}\left[v_r\frac{\mathrm{d}f}{\mathrm{d}r}+f^2-\frac{\nu_\epsilon}{r}\frac{\mathrm{d}}{\mathrm{d}r}\left(r\frac{\mathrm{d}f}{\mathrm{d}r}\right)\right]=0$$

$$\frac{\mathrm{d}}{\mathrm{d}r}\left[v_r\frac{\mathrm{d}g}{\mathrm{d}r}+fg-\frac{\nu_\epsilon}{r}\frac{\mathrm{d}}{\mathrm{d}r}\left(r\frac{\mathrm{d}g}{\mathrm{d}r}\right)\right]=0 \qquad (11)$$

To satisfy the continuity equation, a stream function $\psi(r,z)$ is defined, such that:

$$v_r=\frac{1}{r}\frac{\partial\psi}{\partial z}\equiv\frac{q(r)}{r} \quad \text{and}$$
$$v_z=-\frac{1}{r}\frac{\partial\psi}{\partial r}\equiv-\frac{1}{r}\frac{\mathrm{d}q(r)}{\mathrm{d}r}z+g(r) \qquad (12)$$

where f is given in terms of $q(r)$ by $f(r)=-(1/r)\mathrm{d}q/\mathrm{d}r$.

Defining the dimensionless variable $\eta=(r/R)^2$, where R is the radius of the cylinder, and introducing the expressions (Eq. (12)) into Eq. (11), we obtain for $q(\eta)$ and $g(\eta)$:

$$\frac{\mathrm{d}q(\eta)}{\mathrm{d}\eta}\frac{\mathrm{d}^2q(\eta)}{\mathrm{d}\eta^2}-q(\eta)\frac{\mathrm{d}^3q(\eta)}{\mathrm{d}\eta^3}=0$$

$$\frac{\mathrm{d}}{\mathrm{d}\eta}\left[q(\eta)\frac{\mathrm{d}g(\eta)}{\mathrm{d}\eta}\right]-\frac{\mathrm{d}}{\mathrm{d}\eta}\left[\frac{\mathrm{d}q(\eta)}{\mathrm{d}\eta}g(\eta)\right]=0 \qquad (13)$$

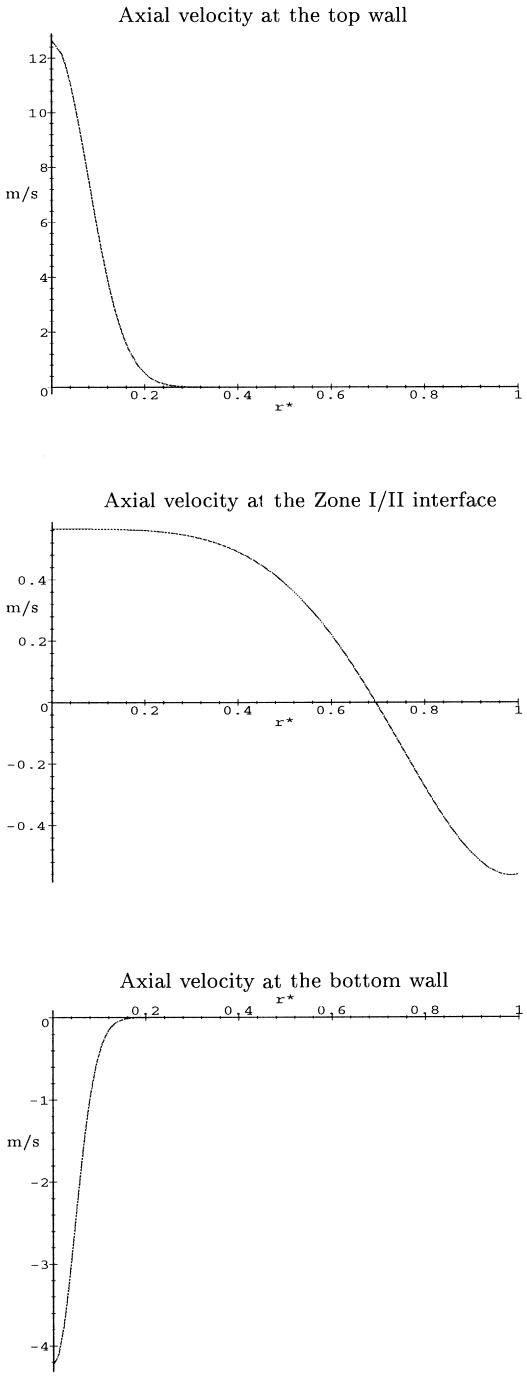

Fig. 4. Simulated axial velocity distribution.

To obtain this equation, that defines the radial and axial velocity, the viscous terms of equation Eq. (11) were neglected. This is the same assumption made by Bloor and Ingham [8], which gave good results for the axial velocity in conical hydrocyclones.

3.2. Boundary conditions

Consider the hydrocyclone divided into two zones. Zone I corresponds to the upper part of the cylinder with a height $L_A=5/4L_V$, where L_V is the length of the vortex finder tube and zone II is the rest of the cylinder with height $L-L_A$, where L is the total height of the hydrocyclone (see Fig. 2).

Assuming that the feed enters through the entire mantel of zone I, the total volume feed rate $Q>0$ is given by $Q=-2\pi RV_R L_A$, from which the boundary condition for $v_r(r)$ in zones I and II are:

$$v_r(R)=\begin{cases}-Q/(2\pi RL_A) & \text{for zone I}\\ 0 & \text{for zone II}\end{cases} \tag{14}$$

The fluid is evacuated from the hydrocyclone through the overflow at the top and through the underflow at the bottom of the equipment at volume rates of Q_o and Q_u, respectively. Both of these are positive numbers. If the radius of the overflow and underflow are designed by R_o, and R_u, respectively, the volume flow at each outlet should be:

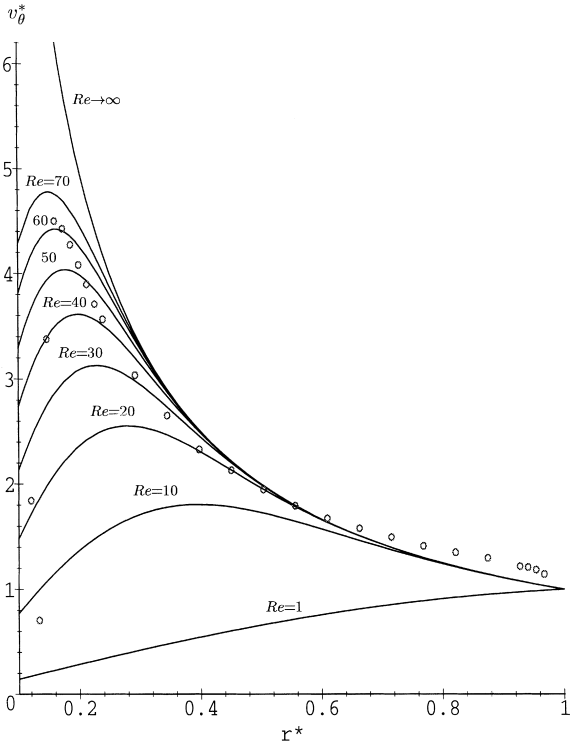

Fig. 5. Dimensionless tangential velocity distribution for several values of the radial Reynolds number, where $v_\theta{}^*=v_\theta/V_{\theta R}$ and $r^*=r/R$. Experimental values correspond to $z^*=0.28$.

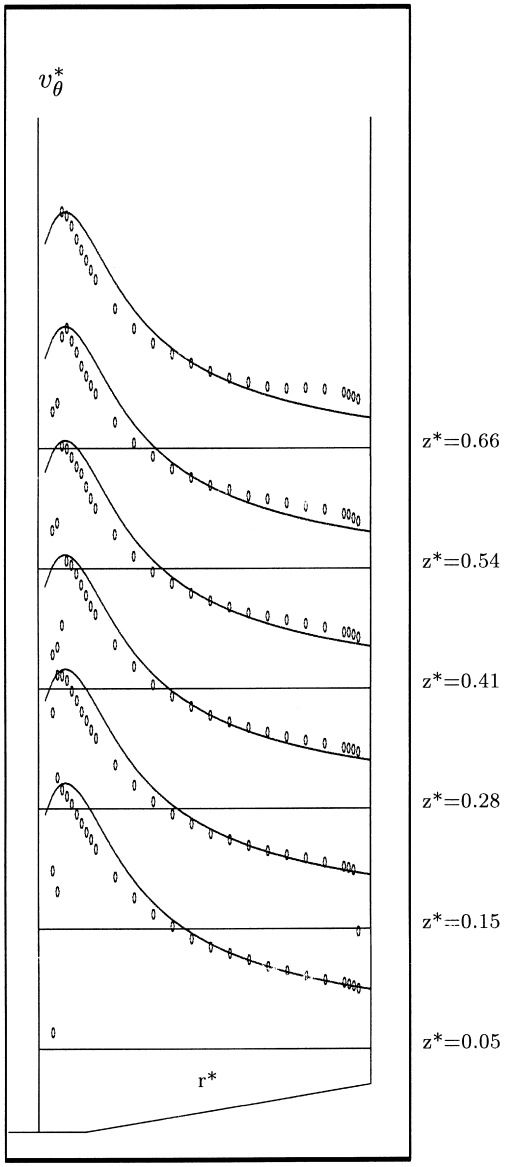

Fig. 6. Comparison of the predicted and experimental dimensionless tangential velocity distribution at several axial levels for Re=65, where $v_\theta{}^*=v_\theta/V_{\theta R}$ and $r^*=r/R$.

$$Q_o=\int_0^{R_o}2\pi r v_z(r,\,z)\mathrm{d}r \quad \text{and}$$
$$Q_u=-\int_0^{R_u}2\pi r v_z(r,\,z)\mathrm{d}r \tag{15}$$

which can be used as boundary conditions for the axial velocity at the top and at the bottom wall.

Consider that the fluid entering the hydrocyclone has a known circulation Γ_R given by $\Gamma_R=2\pi RV_{\theta R}$, then the boundary condition for the tangential velocity is:

$$v_\theta(R)=\frac{\Gamma_R}{2\pi R} \tag{16}$$

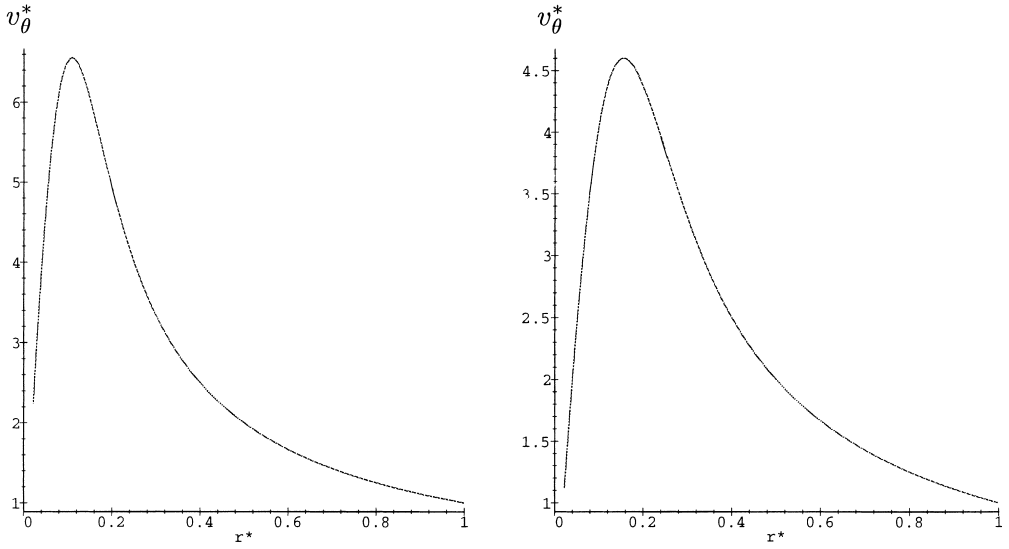

a) Zone I b) Zone II

Fig. 7. Dimensionless tangential velocity distribution of the zones I and II for Re=65, where v_θ*=$v_\theta/V_{\theta R}$ and r*=r/R.

A solution that approximates the set of equations (Eq. (13)) (see Collantes and Concha [9]) is:

$$q(\eta) = \lambda_1(1 - \exp(\lambda_3\eta)) + \lambda_2 \sin(\beta\eta) \tag{17}$$

where β=−(π+arcsin(λ)) with λ=Q_u/Q and with appropriate values for λ_i, i=1, …, 3, which, the same as for $g(\eta)$, are determined depending on the zone.Then,

$$v_r(r) = \frac{1}{r}[\lambda_1(1 - \exp(-\lambda_3\eta)) + \lambda_2 \sin(\beta\eta)] \tag{18}$$

$$v_z(r,\ z) = -\frac{2}{R^2}[\beta\lambda_2 \cos(\beta\eta) + \lambda_1\lambda_3 \exp(-\lambda_3\eta)]z + g(r) \tag{19}$$

Next, the linear differential equation Eq. (9) is solved for v_θ

$$v_\theta(r) = \frac{1}{r}\left[k_1 \int r \exp\left(\frac{1}{\nu_\epsilon}\int v_r(s)\mathrm{d}s\right)\mathrm{d}r + k_2\right] \tag{20}$$

Using the boundary conditions (Eqs. (14)–(16)) and considering each zone separately in such a way that z varies from 0 to L_A in zone I and from 0 to L−L_A in zone II, the following solution was found:

3.2.1. Zone I

$$v_r(r) = -\frac{(1-\lambda)Q}{2\pi L_A r} \times \left\{1 - \exp\left(-\alpha\left(\frac{r}{R_o}\right)^2\right) + \frac{1}{1-\lambda}\sin\left(\beta\left(\frac{r}{R}\right)^2\right)\right\} \tag{21}$$

$$v_z(r,\ z) = \frac{Q}{\pi R^2}\left\{\left[\beta\cos\left(\beta\left(\frac{r}{R}\right)^2\right) + \alpha(1-\lambda)\left(\frac{R}{R_o}\right)^2 \times \exp\left(-\alpha\left(\frac{r}{R_o}\right)^2\right)\right]\frac{z}{L_A} - \beta\cos\left(\beta\left(\frac{r}{R}\right)^2\right)\right\} \tag{22}$$

$$v_\theta(r) = \frac{\Gamma_R}{2\pi r}\,\frac{\{1 - \exp(N_1(r/R)^2)\}}{\{1 - \exp(N_1)\}} \tag{23}$$

3.2.2. Zone II

$$v_r(r) = -\frac{\lambda Q}{2\pi(L - L_A)r}\left\{1 - \exp\left(-\alpha\left(\frac{r}{R_u}\right)^2\right) - \frac{1}{\lambda}\sin\left(\beta\left(\frac{r}{R}\right)^2\right)\right\} \tag{24}$$

$$v_z(r,\ z) = -\frac{Q}{\pi}\left\{\left[\frac{\beta}{R^2}\cos\left(\beta\left(\frac{r}{R}\right)^2\right) - \frac{\alpha\lambda}{R_u^2}\exp\left(-\alpha\left(\frac{r}{R_u}\right)^2\right)\right]\frac{z}{L - L_A} + \frac{\alpha\lambda}{R_u^2}\exp\left(-\alpha\left(\frac{r}{R_u}\right)^2\right)\right\} \tag{25}$$

$$v_\theta(r) = \frac{\Gamma_R}{2\pi r}\,\frac{\{1 - \exp(N_2(r/R)^2)\}}{\{1 - \exp(N_2)\}} \tag{26}$$

where N_1=$\beta Re/2$, N_2=$\beta Re L_A/(2(L-L_A))$ and Re=$-RV_R/\nu_\epsilon$ is the radial Reynolds number. The value for α is selected in such a way that exp(−α)≈0.

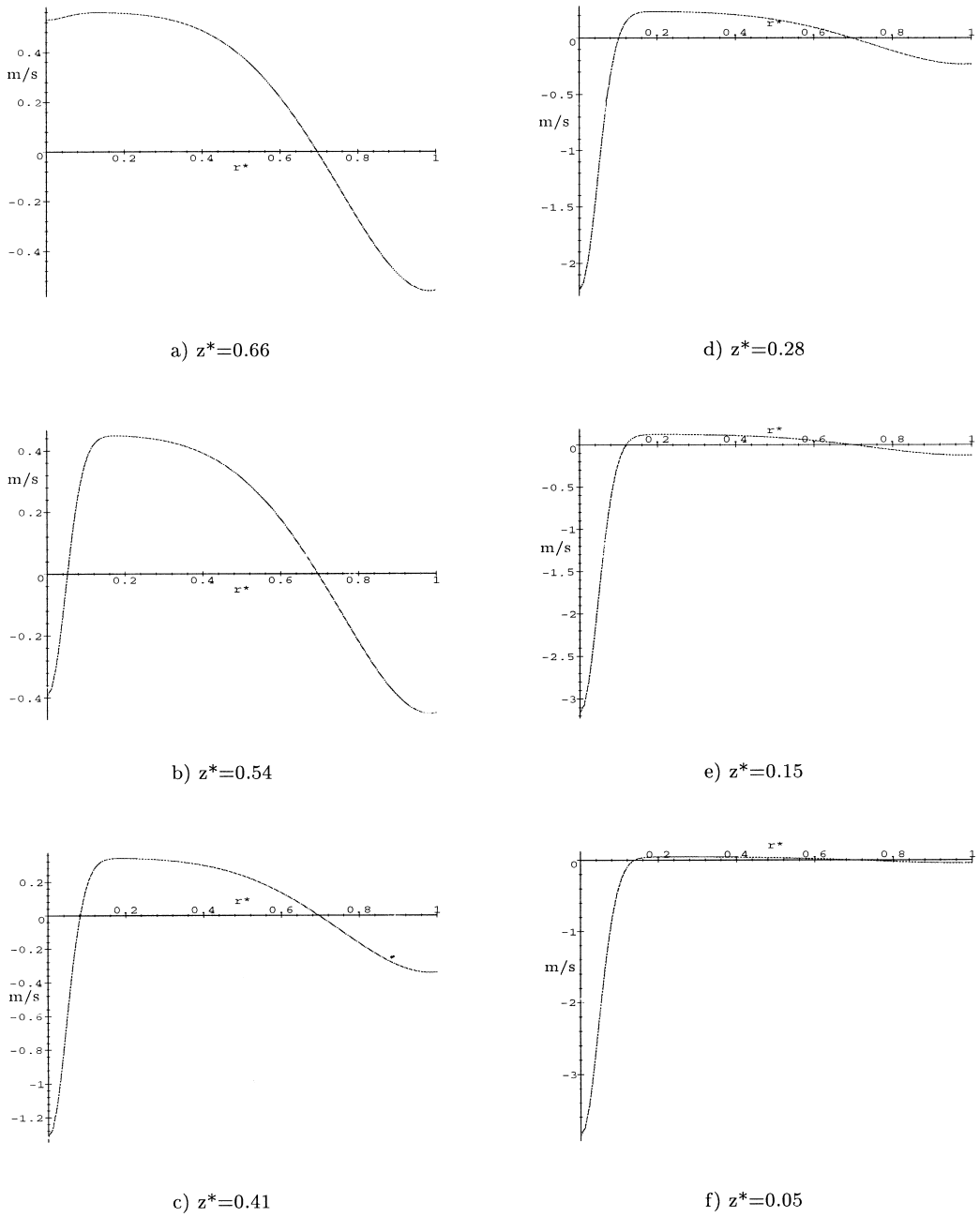

Fig. 8. Axial velocity distribution at different axial levels.

In both the zones g has been selected, satisfying Eq. (13) and considering that $v_z(r,0)$ of zone I is the same as $v_z(r, L-L_A)$ of zone II and that $v_z(r, L_A)$ of zone I and $v_z(r,0)$ of zone II are expressed like exponential functions vanishing outside of the overflow and underflow radius, respectively.

In both the zones the pressure distribution can be calculated from,

$$\frac{p(r,\ z)}{\rho} = \int \frac{v_\theta^2}{r}\,\mathrm{d}r - \frac{v_r^2(r)}{2} - \left(v_r(r)\frac{\mathrm{d}g(r)}{\mathrm{d}r} + f(r)g(r)\right)z - \frac{1}{2}\left(v_r(r)\frac{\mathrm{d}f(r)}{\mathrm{d}r} + f^2(r)\right)z^2 \quad (27)$$

The error of the approximate solution (Eq. (17)) with respect to the exact solution of system (Eq. (13)) is given by the functions f_{1j}, j=1, 2 at zone I and f_{2j}, j=1, 2 at zone II. These functions are defined by,

$$f_{11}(\eta) = \left\{\lambda_2(\lambda_3^2+\beta^2)[\beta\cos(\beta\eta)+\lambda_3\sin(\beta\eta)] + \lambda_1\lambda_3^2\right\} \times \exp(-\lambda_3\eta) - \lambda_2\beta^3\cos(\beta\eta) \quad (28)$$

$$f_{12}(\eta) = \{(\lambda_3^2+\beta^2)\exp(-\lambda_3\eta) - \beta^2\}\cos(\beta\eta) \quad (29)$$

$$f_{21}(\eta) = \{\lambda_2(\lambda_3^2+\beta^2)[\beta\cos(\beta\eta)+\lambda_3\sin(\beta\eta)] + \lambda_1\lambda_3^2\} \times \exp(-\lambda_3\eta) - \lambda_2\beta^3\cos(\beta\eta) \quad (30)$$

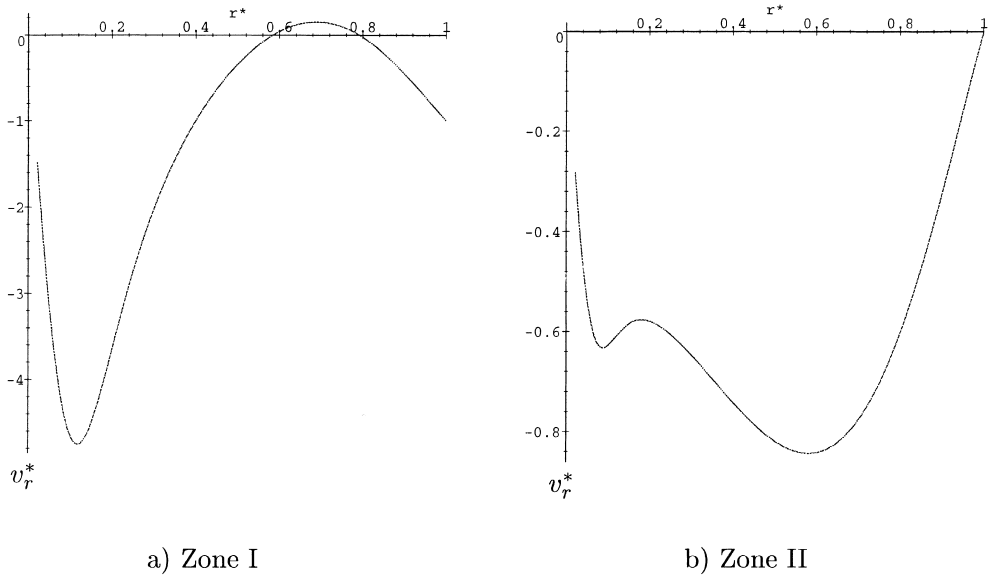

Fig. 9. Dimensionless radial velocity distribution of the zones I and II, where $v_r{*}=v_r/V_R$ and $r{*}=r/R$.

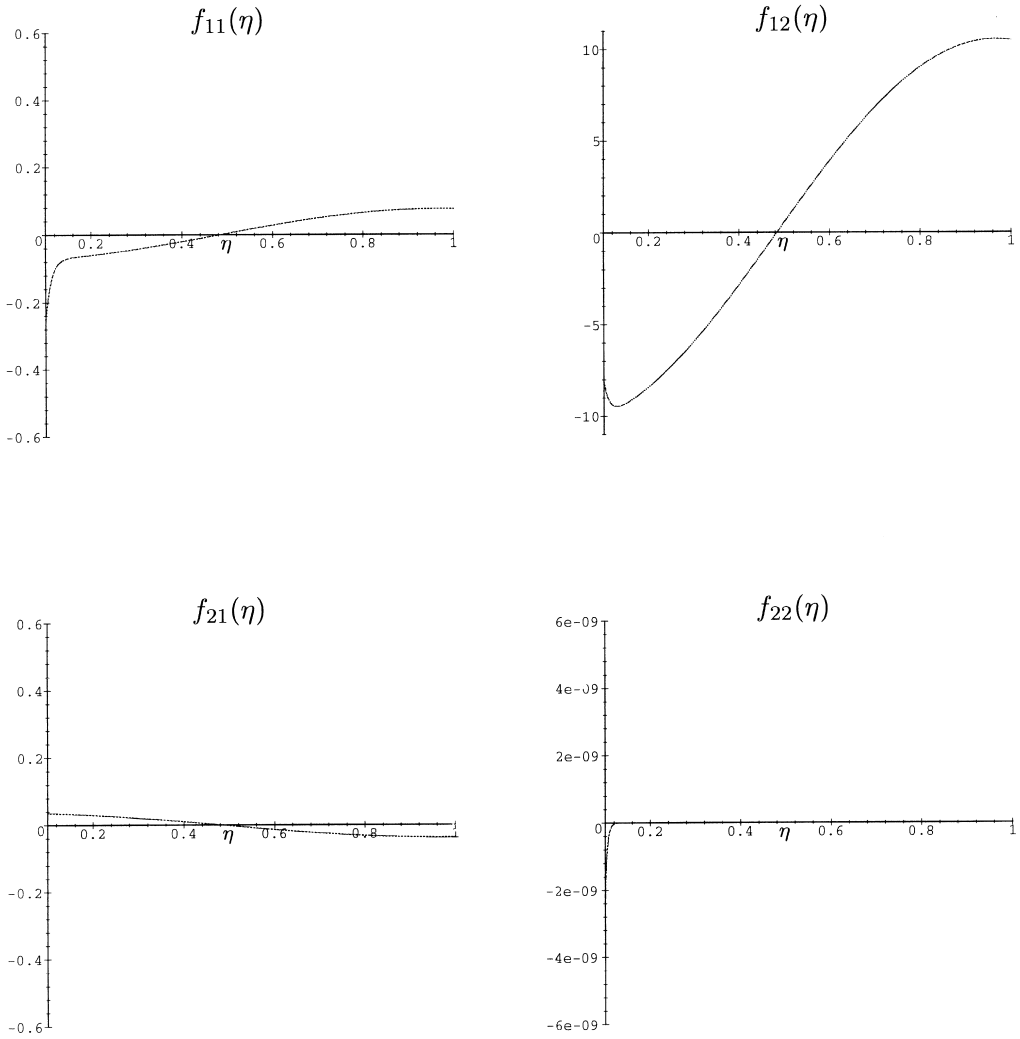

Fig. 10. Error of the approximate solution.

$$f_{22}(\eta) = \{\lambda_2(\lambda_3^2 + \beta^2)\sin(\beta\eta) + \lambda_1\lambda_3^2\}\exp(-\lambda_3\eta) \quad (31)$$

In Eqs. (28) and (29) λ_i, i=1–3 correspond to their values in zone I and in Eqs. (30) and (31), to their values in zone II.

4. Results and discussion

Heights of the zones I and II are arbitrary. We selected L_A=5/4L_V since, from the experimental results, we have symmetric velocity distributions at this height. The first set of experimental velocity values is just below of the zone I/II interface selected in this way.

The external tangential velocity at the wall $V_{\theta R}$ was considered to be the lowest velocity of the experimental tangential velocity values near the wall at the different axial levels.

Fig. 3 shows a comparison of predicted axial velocity using equation Eq. (25) and experimental values. Although the radial dependence of v_z, is fairly represented, the overall representation of the axial velocity is satisfactory. Fig. 4 shows the shape of v_z, at the overflow, underflow and at the zone I/II interface.

The variation of the tangential velocity with the Reynolds number is given in Fig. 5 and it is similar to that obtained by other research workers. As a result, the value of Re=65 was selected as appropriate to match experimental results. Comparison of the experimental tangential velocity and that simulated with Eq. (26) for several heights in the hydrocyclone is given in Fig. 6, with satisfactory results.

Fig. 7 shows the solution for the tangential velocity in the zones I and II. Moreover, the variation of the axial velocity at different heights of the hydrocyclone is shown in Fig. 8. Fig. 9 shows the prediction of the radial velocity in the zones I and II.

Finally, Fig. 10 shows the error of the approximate solution Eq. (17). As is seen in the subfigures, it is a very good approximate solution in zone II, which is the zone of great importance for particle classification. The modeling of zone I is given to complete the axial symmetric model, but it only gives an idea of what might occur in this zone.

5. Conclusions

From the exact solutions of the Reynolds equations, as given in this work, and from the results of other research workers that have modelled the cylindrical hydrocyclones [10], we can say that in a cylindrical hydrocyclone, the radial velocity depends strongly on the shape of the axial velocity. One can obtain completely different radial velocities distributions by choosing appropriate axial flows. Nevertheless, the shape of the tangential velocity, as a combination of a free vortex and a rigid motion, is insensible to the form of these axial and radial velocities. It is important to note that non of the radial velocities chosen by Rietema [1,2,5] or Upadrashta [11] can have associated axial velocities that resemble the experimental ones. All of them require that the axial flow enters axially into the hydrocyclone.

For the axial velocity to be a consequence of the radial velocity, it must be a function of r and at least a linear function of z. Finally, we can indicate that, in modelling the hydrocyclone, the selection from several solutions to the field equations by comparing the size of the maximum of the tangential velocity with experimental values, is not the proper way to go. The three, or at least two velocity components must be compared and specially the axial velocity must be reasonable.

Acknowledgements

The authors acknowledge the partial financial support of this work by the following institutions, DAAD through project 429-511-010-7/334-400-031; Fundación Andes through project C-13131; FONDEF through project D97-I2042; National University Pedro Ruiz Gallo, Perú, where the first author is Staff member and United Engineering Foundation through a fellowship to participate in the Conference on solid–liquid separation, Hawaii, 18–23 April, 1999. The present work is part of the D.Sc. thesis in Mathematical Engineering of the first author at the University of Concepción, Chile.

References

[1] K. Rietema, H.J. Krajenbrink, Theoretical derivation of tangential velocity profiles in a flat vortex chamber. Influence of turbulence and wall friction, Appl. Sci. Res. 8 (1958) 177.
[2] K. Rietema, Performance and design of hydrocyclones: I. General considerations, Chem. Eng. Sci. 15 (1961) 298.
[3] G. Van Duijin, K. Rietema, Performance of a large-cone angle hydrocyclone, I. Hydrodynamics, Chem. Eng. Sci. 10 (1983) 1651.
[4] D.F. Kelsall, A study of the motion of solid particles in a hydraulic cyclone, Trans. Inst. Chem. Eng. 30 (1952) 87.
[5] K. Rietema, Liquid–solids separation in a cyclone: the effect of turbulence on separation, Symposium on the Interaction Between Fluids and Particles, London Inst. Chem. Eng., 1962, p. 275.
[6] F. Durst A. Melling J.H. Whitelaw (Eds.), Principles and Practice of Laser Doppler Anemometry (1981) 342Academic PressLondon.
[7] C.P. Donaldson, R.D. Sullivan, Behavior of solutions of the Navier–Stokes equations for a complete class of three-dimensional viscous vortices, Proceedings of the Heat Transfer and Fluid Mechanics Institute, 1960, p. 16.
[8] M.I.G. Bloor, D.B. Ingham, Boundary layer flows on the side walls of conical cyclones, Trans. Inst. Chem. Eng. 54 (1976) 276.
[9] J. Collantes, F. Concha, Vortex flow in flat bottom hydrocyclones: zero order approximation, Technical report 98-12, Mathematical Engineering Department, University of Concepción, Chile, 1998.
[10] F. Concha, Phenomenological Modeling of hydrocyclones, Plenary Lecture, Engineering Foundation Conference on Solid–Liquid Separation, Hawaii, 18–23 April 1999.
[11] K.R. Upadrashta, V.J. Ketchman, J.D. Miller, Tangential velocity profile for pseudoplastic power-law fluids in the hydrocyclone — a theoretical derivation, Int. J. Miner. Proc. 20 (1987) 309.